

Brazilian coast has a very narrow and consequently very steep slope. The BC, NBC, and the Malvinas Current comprise the main conduits for exchanging the oceanic information between the distinct regions, including heat, freshwater, biogeochemical properties, dissolved matter, larvae, etc. (D'Agostini et al., 2015; Endo et al., 2019; Saraceno et al., 2005). The local oceanic circulation, air-sea interaction processes as wind, heat flux and precipitation, and physical features such as the coastline orientation and topography make each region by themselves unique cases for water properties distribution, biological speciation, productivity, etc.

Nutrients and productivity for the region could also come from an oceanic source, that is the case when there is an intrusion of a water mass such as the South Atlantic Central Water (SACW). It can usually be found at the continental slope depths between 100 and 500 m (Stramma & England, 1999). Under proper wind conditions, the prevalence of wind stress parallel to the coast gives rise to vertical displacements of water volume and thus change the surface temperature and nutrients distribution (Brandini et al., 2014; Castelão et al., 2004; Cerdá & Castro, 2014; Palma & Matano, 2009). Changes in the volume transport intensity by the western boundary currents and in its mesoscale features could alter the intrusion of the oceanic water masses into the shelf, also influenced by the wind patterns.

Studies have shown the impact of some of these major features along the South American coast. Ghisolfi et al. (2015) explored the different oceanographic conditions that affect the water column stratification and nutrient supply for the primary production over the eastern Brazilian shelf. Whereas in the northern portion of the Abrolhos and adjacent banks there are more momentum input and properties induced by eddies and meanders of the BC, in the southern portion, the more sheltered area is susceptible to an advective mixing caused by the vertical current shear associated with changes in wind direction or intensity. The aforementioned banks affect the BC mean flow, leading to mesoscale instabilities and meanders that impact significantly the circulation of the regions toward the south (Calado et al., 2008; da Silveira et al., 2008). In the southern region of our study area, Piola et al. (2008), Garcia and Garcia (2008), Machado et al. (2013), Guerrero et al. (2014), Matano et al. (2014), Mendonça et al. (2017) indicated the extent and influence of the La Plata plume to the sea surface salinity and the chlorophyll concentrations over the Brazilian shelf associated with surface winds and river discharge. Similarly, Moller et al. (2010) showed that the wind field works as a regulator of the Amazon River plume's northwestward flow and observed that the ocean surface currents, especially the NBC, are the main factors influencing river plume dispersion patterns in the shelf.

Our hypothesis is that large-scale, low-frequency, open-ocean processes influence regions along the eastern South American shelf, and that topography and freshwater discharge of large rivers can constrain and modify the response to these processes. The continental shelf is connected by advection provided by the main western boundary currents; mesoscale and shelfbreak eddies, coastal upwelling and inertial currents introduce variability to the spectrum on shorter temporal and spatial scales. In that, our focus is on the total variability that arises from the combined effect of advective and local processes, that is, the effects and not the mechanisms themselves. We aim to explore these regional similarities along the coast in terms of three oceanic variables using satellite data: sea surface temperature, salinity, and chlorophyll-a concentration. The influence of the open-ocean processes was quantified in terms of the spatial and temporal extension of the signals with similar phase, and/or similar spectrum for the three variables. The analysis was done with data selected along smooth continuous paths that follow isobaths along the coast, keeping track of key geographic locations often cited in the literature. We start with the characterization of the annual signal, proceeding with the anomalies analysis relative to it. These include Hovmöller (space-time) diagrams, isobath-following spectra, decomposition by a filter chain, and correlation with climate indices. The main novelties of our approach are that: (1) we used the same framework of simultaneous spatial and temporal analysis to cover approximately 9000 km of ocean, following isobaths that are characteristic of different regions of the continental shelf; (2) we quantified the annual signal in detail, removed it, and proceeded to examine changes to the spectral content along the coast as one moves offshore; (3) the correlation with climate indices was performed at the key locations using exactly the same method and data.

2. Data and Methods

We analyzed time series of sea surface temperature (SST, °C) from the level-3 Moderate-resolution Imaging Spectroradiometer (MODIS)/Aqua sensor with a 4 km spatial resolution and monthly resolution, from August 2002 until January 2019 NASA/JPL (2020). The chlorophyll-a concentration (CHL) product (mg m^{-3}), also from

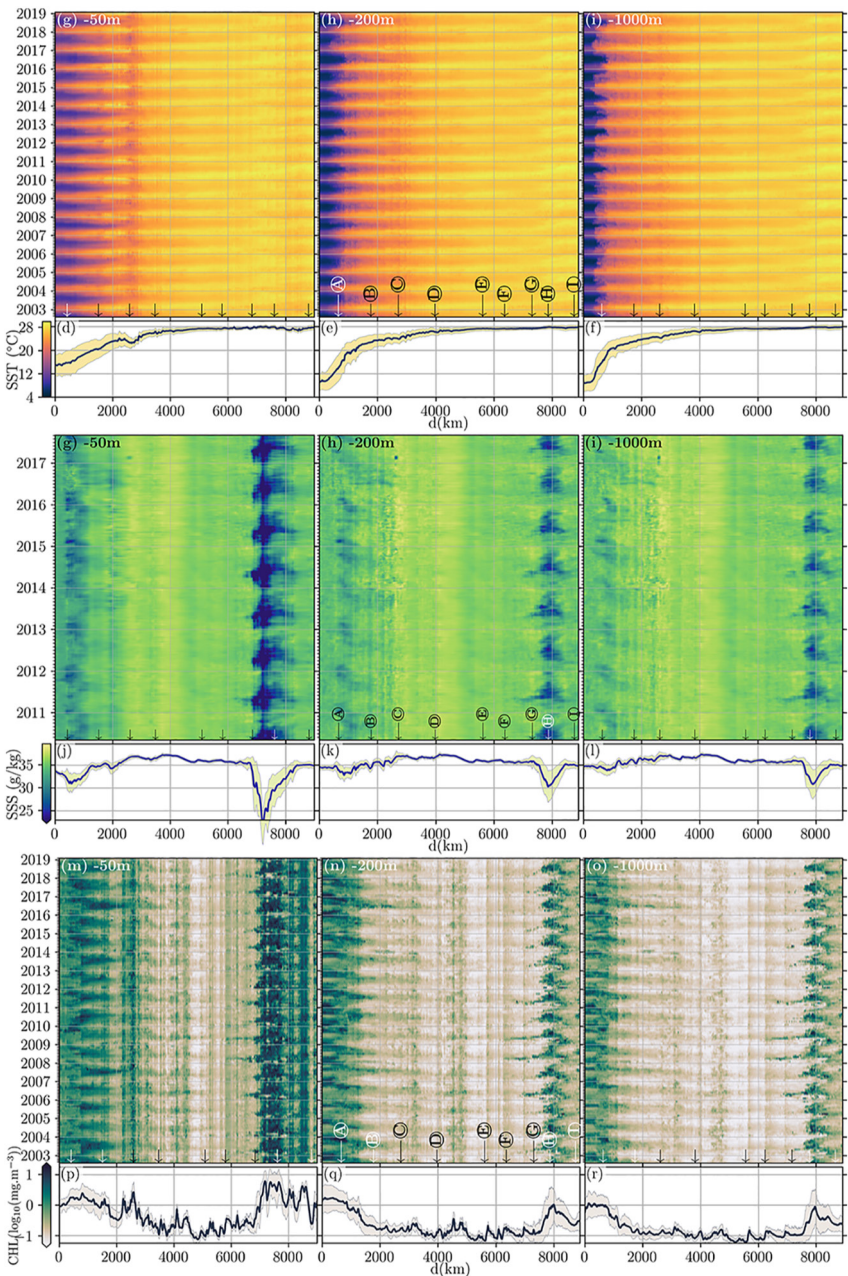


Figure 2. The original SST (a–c), SSS (g–i) and CHL (m–o) are presented as colored space-time diagrams, with the isobaths referenced in each top left corner. The abscissae represents the distance d along the isobaths, counted from the southernmost point of the dashed-red lines in Figure 1. The corresponding lower panels represent the mean (solid line) and the standard deviation (shaded area) as a function of distance.

is the reach of the seasonal signal relative to the distance along the isobaths. For instance, for the -50 m isobath, most of the points south of Cabo Frio have a similar seasonal cycle amplitude A (and σ), covering a distance over 2500 km from the origin, however at the -1000 m isobath, regions with similar amplitudes just reach as north as the La Plata River (A).

The along-shore colder temperatures in shallower isobaths on the northern part of the SBB are caused by the inner-shelf intrusion of the SACW coming from Cabo Frio (C) region with southwestern extensions of 100–300 km during austral winter, spring, and summer (Cerde & Castro, 2014). This phenomenon is predominantly controlled by the year-long shelf-break upwelling and seasonal offshore Ekman transport. The former is governed by the

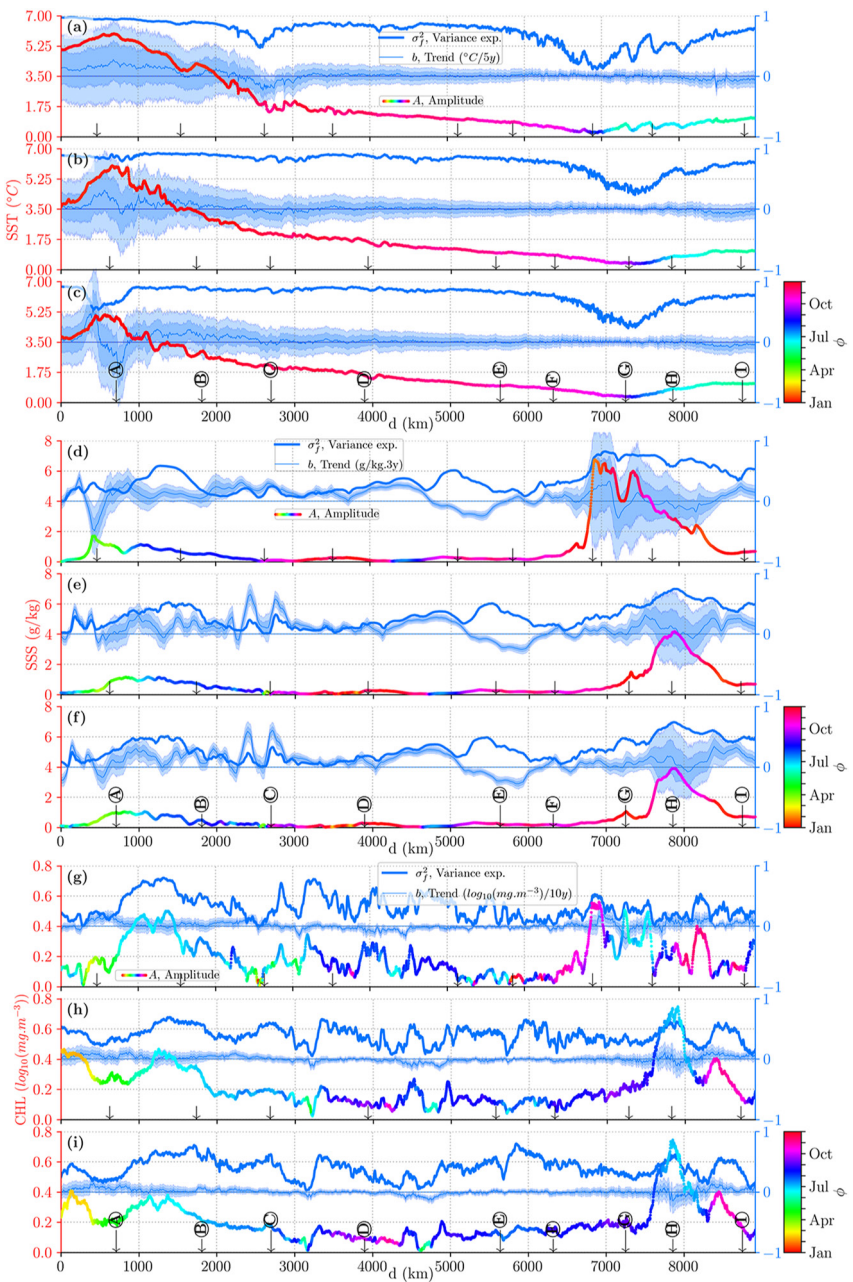


Figure 3. Amplitude (left axis) and phase of the seasonal cycle (multicolored lines and colorbar), fraction of variance (σ_f^2) (thicker blue lines), and trends (lighter blue) with the corresponding 68% and 95% confidence intervals as shading areas of SST (top), SSS (middle) and CHL (bottom) at the -50 , -200 , and -1000 m isobaths (both blue curves use the right axis).

from Equation 1, in that a cosine was adjusted. Thus, $\Phi = 0$ indicates a maximum in January 1 and it is represented by red; a smooth color transition occurs over the equator. The maximum of the seasonal cycle occurs in summer: around December/January at the southern hemisphere and June/July at the northern side. In the vicinity of large rivers, the amplitude increase is at least partially due to the contribution of the contrasting temperatures of river discharges. Near the Amazon River (G), for instance, Ffield (2005) and Neto and da Silva (2014) showed that the SST spatial distribution follows the seasonal variability of the river plume, with higher SST ($>28^\circ\text{C}$) waters spread along the north Brazilian shelf when the river discharge is high and the NBC is low (May and June). Whilst during July and August, a cold tongue ($<27.5^\circ\text{C}$) associated with the increased NBC flow is observed south of 3°N , with the river warmer waters restricted to the inner continental shelf and north of 6°N . However,

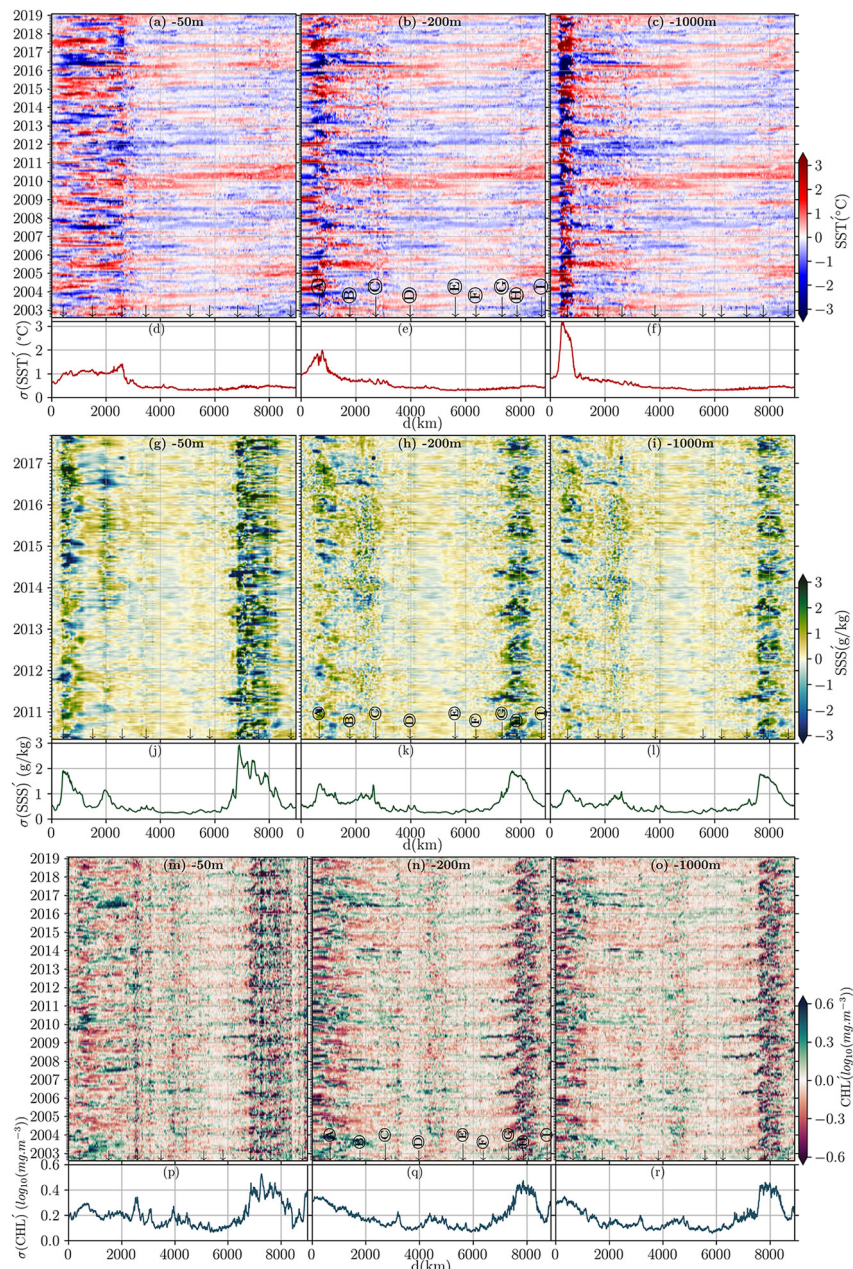


Figure 4. Space-time diagrams for the SST' (top), SSS' (middle), and CHL' (bottom) anomalies relative to the annual cycle and trend, and their respective standard deviation as a function of distance along the -50 , -200 , and -1000 m isobaths.

The SST' shows striking large scale patterns in all isobaths where signals connect the coast from north to south (Figures 4a–4c). For instance, there is a strong positive (red) anomaly departing from Cabo Frio (C) in 2009–2010 whose intensity can be followed to the northernmost point up to 2011. Two years later a negative (blue) anomaly follows the same pattern. A longer positive event occurred in Jun 2015–Jun 2017 spanning the three southernmost locations in Figure 4a, and reaches the northernmost locations in 2016–2018. Again, it is followed by a negative event, and both positive and negative events seem to be delayed at location (C). The SST' Hovmöller diagrams reveal a series of highs and lows in intervals ranging from 2 to 4 years. To explore the impact of these interannual changes, the analysis of Figures 4 and 5 combined is more effective. In the Hovmöller diagrams of Figure 4, each vertical slice is a time series taken at location d ; these are anomalies, in the sense that the mean, trend and

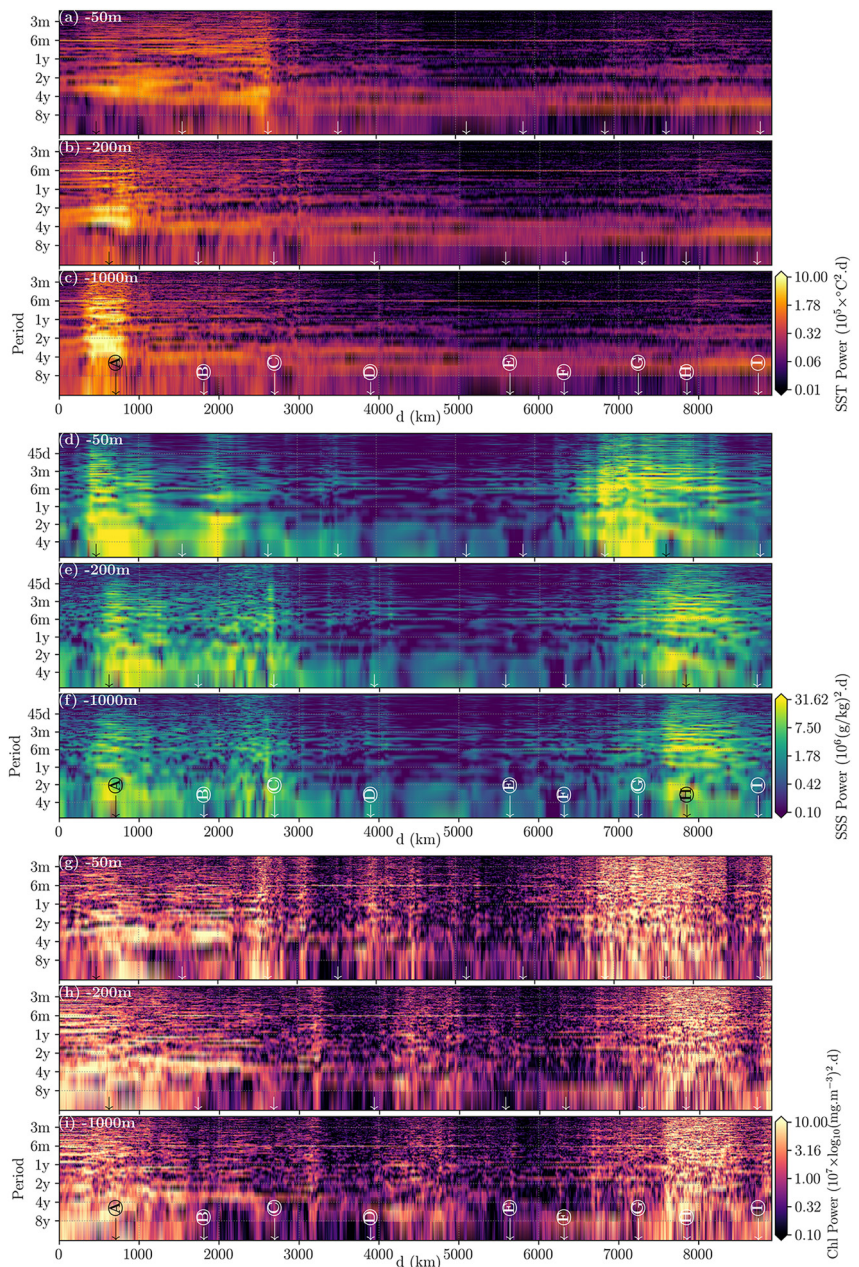


Figure 5. Variance preserving power spectrum density as a function of location, for all variables. Panels a–c are for SST', d–f for SSS', and g–i for CHL'. Each triplet uses one color bar.

annual cycle were removed (Equation 1). Consequently, their spectra, shown in Figure 5 as a function of the same location d , has no annual signal.

The SST' power spectral density (Figures 5a–5c) shows that the spectral power is, on average, larger on the southern part of the study area, and these maxima are more intense (light yellow) in the deeper isobaths. In comparison, over the -50 m isobath the region with relatively high power spreads to the north, up to Cabo Frio (C). This suggests that part of the energy from the region near (A) propagates inshore and reaches the inner shelf. Most of these signals are horizontally aligned in Figures 4a–4c, indicating that the time scale of this process is often similar to our temporal resolution, on the order of a month. That temporal scale is similar to the time interval taken by the Lagrangian drifters in de Souza and Robinson (2004) to cross the distance from (A) to (B). It is possible that the SST' signal is advected by the Brazil Coastal Current (BCC). From Figure 4a (and to a lesser

those locations are close to the geographic location of the areas used to compute the indexes used here. That is the case of TNA, TSA, SAODI, and AMO.

AO and NAO's correlations with SST' at a 4-year window are higher in the northern part of the basin, from E to I. Correlations with AO are slightly higher and more significant than for NAO. Similarities between the correlations are expected because both indices are correlated with each other (Wallace, 2000), that is, the phases of NAO and AO often coincide. One of the impacts of their positive (negative) phase is the intensification (weakening) of the northeast trade winds in the tropical North Atlantic due to the intensification (weakening) of the North Atlantic Subtropical high-pressure system. Consequently, there is a cooling (warming) of the ocean surface through the increase (decrease) of the latent heat flux loss to the atmosphere, according to wind-evaporation-SST feedback (Chang et al., 1997; Czaja et al., 2002; Xie & Philander, 1994). Therefore, the negative correlations of the NAO and AO with SST' on the north coast of Brazil can be explained by the changes in the northeast trade winds.

The correlations of SST' and the indices calculated in the Southern Hemisphere (TSA, SAODI, and AAO) are significant and their effects can be seen widespread in the array. Furthermore, PDO and Niño 3.4 show a significant impact on the southeastern part of the Brazil coastline, from Cabo de Santa Marta (B) to Abrolhos (D) with correlations at 95% confidence level. Several studies have investigated the influence of Pacific climate indices in the South Atlantic Ocean. For PDO and El Niño, the mechanism that explains this connection is the propagation of extratropical atmospheric Rossby waves (Cai et al., 2020; Grimm, 2003; Lopez et al., 2016; Reboita et al., 2021; Rodrigues et al., 2015). However, these are mechanisms at a large scale, and they modify the ocean primarily through local modification of the winds. As we found significant correlations (>51%) for specific regions (B, C, and D for SST' and only A for CHL'), we emphasize the importance of further studies in explaining the local impact of these mechanisms. Although our results indicate statistically significant correlations, the length of our time series is not long enough to contemplate the PDO's multidecadal variability. Therefore, any conclusions related to that index should be taken cautiously.

Compared to SST and CHL, the SSS time series are much shorter therefore the correlations at interannual scales may not be significant depending on the considered index. Another point, probably the most important, is that salinity patterns are locally driven, as we have concluded when examining the shorter seasonal-scale variability. However, climate indices also influence local aspects like river discharge. For instance, the La Plata River has an increase (decrease) in its flow due to an increase (decrease) in the rainfall at the La Plata basin during El Niño (La Niña) events (Ciotti et al., 1995; Tedeschi et al., 2013). This observation is an indication that the effects of atmospheric teleconnections on SSS along the South Atlantic western boundary are not trivial and require further study. Finally, the correlations with CHL' were only significant at fewer locations compared to SST'. Some of the highest correlations are related to sites that are not directly influenced by river discharges. Compared to SST', CHL' correlations are smaller, only significant at certain locations and they can hardly be observed along a large extension.

4. Concluding Remarks

Our main goal was to obtain a large-scale perspective of the processes that occur from near the coast up to an offshore distance under the open ocean influence and from the south to the north of the South American coastline, from satellite-derived variables. Regional circulation patterns and biological processes often change as one moves away from the coast. The distinction between regions is marked by the diversity of local regimes: sometimes dominated by river discharges, topographic features or large-scale atmospheric and oceanic contributions. We envision this work to be useful as a reference for those who are interested in quantifying the relation between physical and biological parameters along the coast and their relationships in time and space.

Our investigation involved connecting an array of points along the coast. Rather than selecting points at a constant distance from the coastline, we chose to use the local layer thickness of the ocean as a criterion. Locations that fall near the isobaths of -50 , -100 , -200 , -500 , and -1000 m were selected, from those -50 , -200 , and -1000 m are discussed. The array extends from the La Plata River in the south to the Essequibo River in the north of the South American continent. Sea surface temperature (SST), sea surface salinity (SSS), and chlorophyll-a concentration (CHL) were obtained at those locations. Each point presented a time series from 2002 to 2019 for SST and CHL, and from 2011 to 2017 for SSS. That selection allowed us to build space-time diagrams that show the evolution of features along the years or help us to perceive whether closeby regions present covariant patterns.

